# Advanced Sliding Mode Control with Disturbance Rejection Techniques for Multi-DOF Robotic Systems

Mohamed Abdelhakim Basal [1*]
[1] Faculty of Engineering, Menoufia University, Egypt
Email: [1] mohamedabdelhikeem@yahoo.com
*Corresponding Author

***Abstract*—For the control of complex and non-linear systems such as robotic arms, especially in sensitive systems such as medical applications and chemical industries, it becomes necessary to improve the performance considering the balance between fast response and smooth, vibration-free, in addition to overcoming disturbances and model uncertainty. These and other reasons may be the reason for the failure of some linear and classical control systems. This research presents a hybrid control system that combines sliding mode control (SMC) with an active disturbance rejection controller (ADRC) for a three-degree-of-freedom (3-DOF) robotic arm. The research contributes to developing a robust control system that reduces the vibrations caused by the classical SMC and utilizes its advantages to achieve smooth, fast, high dynamic response. The proposed method combines the benefits of SMC stiffness for regulating the angular velocities and ADRC in disturbance compensation to regulate the angular positions, ensuring smooth and accurate control despite its relative complexity. The simulation results show that the classical SMC methodology provides superior performance compared to the traditional PIDC in terms of low settling time, but suffers from higher overshoot and large vibrations that sometimes cause a large value of tracking error. In contrast, the proposed control methodology contributes to the improvement of the robotic arm performance, achieving higher tracking accuracy, tracking error minimization, very low settling time, and clear vibration cancellation in both the output signals and the applied control signals. The proposed system has clear advantages, so it can provide a promising solution for robotic arms, particularly in industries demanding high performance, fast tracking and minimal vibrations.**

***Keywords*—3-DOF Robotic Manipulator; Sliding Mode Control; Disturbance Observer Design; Tracking Error Minimization; MATLAB/Simulink.**

## I. INTRODUCTION

Manipulative robotic arms are gaining increasing popularity due to their excellent performance and ability to perform tasks accurately and quickly in various applications. In addition, robotic arms contribute to reducing errors and improving the quality of industrial processes. These applications include multiple tasks such as picking and placing materials in specific locations, welding processes, automated painting, and automatic assembly of electronic and mechanical components. Automotive, aerospace, medical, and even research and home applications. This diversity of uses reflects the flexibility of these systems and their ability to meet the requirements of precise and complex tasks [1]-[11]. Achieving efficiency in these processes requires advanced control strategies that ensure precise coordination between different degrees of freedom, with the ability to handle different loads and adapt to changing conditions [12]-[18].

Robotic arm control engineering focuses on designing controllers that perform at the highest quality, with high dynamics and stability, and achieve the lowest tracking error. To improve stability and performance, advanced controllers and various modern technologies are used, such as enhanced proportional-integral-differential (PID) controllers or PID controllers integrated with intelligent control technologies [19]-[29]. This is because classical control systems only cover linear systems; in addition to that, they suffer from some drawbacks, such as low dynamics and may not be effective for multiple-input, multiple-output (MIMO) systems.

The state feedback methods like linear quadratic regulator (LQR) are an effective solution for controlling MIMO systems, improving the system performance and stability, it has been used in a number of published literature for robotic and manipulator systems such as in [30]-[37].

Modern control systems for robotic and manipulator systems have proven their effectiveness in providing high stability and reliable dynamic performance even in the presence of various disturbances or uncertainties and changes in system parameters. These systems include different techniques such as nonlinear control systems such as sliding mode control (SMC) [38]-[41] and back step control (BSC) [42]-[45], artificial intelligence techniques (AIT) such as fuzzy logic and neural network [46]-[49] and other approaches such as active disturbance rejection controller (ADRC) [50]-[54] or fractional proportional-integral-differential (FOPID) control systems [55], [56].

The hybridization of control systems is very effective in obtaining high stability and dynamic performance while maintaining a static error at a minimum value without the presence of various defects such as vibration or being affected by various disturbances, despite the control system design being based on a questionable model or the presence of various other challenges. Therefore, much research has been done in this regard, such as [57] which proposed an adaptive fuzzy control system for a three-degree-of-freedom hydraulic arm position, designed to handle large load

variations. The system combined backscatter-based slip control, a fuzzy logic system, and a nonlinear disturbance controller. The slip control adjusts the dynamics of the arm and actuators, while the fuzzy logic is used to adjust the control gain based on the output of the disturbance controller, allowing for effective compensation of load variations. A two-link arm control methodology is proposed in [58] that includes the design of a nonlinear disturbance controller supported by a neural network, using an integrated sliding manifold and backtracking techniques to ensure the system's efficiency and stability. In [59] the dynamics model is precisely compensated in the SMC by proposing a parallel artificial intelligence network. In [60], a control algorithm based on fuzzy logic and SMC was presented to address the control errors and input jitter problem encountered by conventional control methods for controlling underwater manipulators. One common type of robotic controller is the three-degree-of-freedom (DoF) articulated controller. It typically has three rotary joints, allowing for three-dimensional movement. Tasks requiring simple spatial positioning, such as pick-and-place actions, simple assembly tasks, vehicle assemblies, or educational purposes, frequently require this type of controller. Based on the structure of this arm, it is characterized by the following [61]-[70]:

1) Articulated structure: A large range of motion is provided by the arrangement of the joints in a chain.
2) Three degrees of freedom: Three levels of motion can be performed using the three rotary joints, which typically correspond to:
   a. Base rotation.
   b. Shoulder movement.
   c. Elbow movement.
3) Workspace: The end controller can reach positions within a certain range and direction thanks to the spherical workspace of the design.

By reviewing some of the published literature on controlling this type of arm-robot, it was found that during the two researches [61], [62], an LQR methodology was used to regulate the angular positions of the three joints, while in the research [63], the performance of LQR was improved by using adaptive control techniques. In [64], [65], a state feedback control system and PID regulators were used to track the path in three-dimensional space. In line with this goal, the authors in [66] designed controllers using neural networks to improve the positioning and orientations of the end effector and simplify the forward and Inverse Kinematics relationships. In [67], a robust Hinf controller was designed based on a simplified model of the arm-robot and the results were compared with PID controllers, with only the logarithmic features of the results being presented. In [69], the sliding mode technique is used to improve the tracking of the angular positions of the three joints, relying on the optimization algorithm to adjust the parameters of the control system.

Some of the drawbacks of different control techniques used in previous literature can be summarized as follows:

1. PID-based control systems may fail to control some complex multi-degree-of-freedom robot systems when the performance criteria are stringent and strong, especially when the number of inputs does not match the number of outputs or when strong coupling effects exist between different variables.
2. LQR-based control systems performance may not be adequate as it has a linear control law like PID controller.
3. Using control systems based on a specific technology may cause the control system to lose some of the positive advantages offered by another technology. It is known that the sliding mode control system is characterized by strength and robustness, but it suffers from the phenomenon of chatter. In contrast, the backstepping control system may not provide the same robustness as the sliding mode, but it is characterized by the absence of vibrations. Also, some control systems, such as FOPID, AIT, and Hinf controllers suffer from a high degree of computational complexity, difficulty in practical implementation, and the need for extensive calibration and adjustment to obtain strong and effective performance.

Considering the above-mentioned drawbacks and the importance and effectiveness of hybrid control systems for robotic arms mentioned in [57-60], this research aims to design a hybrid control system based on SMC and ADRC controllers that has a lower degree of complexity compared to other hybrid systems and achieves efficient performance and high dynamics to overcome various disturbances and achieve efficient and continuous tracking of reference values.

### *A. Contributions that the Research Seeks to Achieve*

In systems with sensitive missions such as medical applications, chemical industries, and aviation systems. Tracking speed and accuracy are of utmost importance, but a balance must be struck between fast response and vibrational response. In addition to improving overall performance in terms of reducing tracking error and overcoming various disturbances that may result from model non-linearity or uncertainty. The research contribution focuses on developing a robust control system that combines SMC and ADRC, and is characterized by the following:

a. Efficient performance: enhancing the system's time response characteristics (reducing both settling time, overshoot and steady-state error).
b. High dynamics: ensuring that the control system responds quickly and smoothly to time-varying reference signals (tracking a circular path for example).
c. Disturbance rejection and uncertainty overcoming: dealing effectively with various disturbances, and ensuring robust operation despite the inaccuracy of the mathematical model adopted during the design of the control system.
d. Reference tracking: maintaining accurate and effective tracking of the required reference values, even in difficult conditions.

*B. Structure of the Paper*

The rest of this paper is organized as follows. Section 2 describes the dynamic model of the robotic arm, and also presents the linear model of it, which is essential for the design of the proposed controllers. Section 3 discusses the strategies of the control systems. Section 4 presents the simulation results comparing the performance of different control strategies. Finally, Section 5 concludes the paper by summarizing the results and suggesting future research directions.

## II. System Description and Dynamic Model [63]-[70]

Robotic arms have become a cornerstone of modern automation and industrial applications. The depicted robotic arm consists of multiple articulated joints as shown in Fig. 1, each allowing rotational motion around specific axes. This design enables the arm to perform precise and complex movements within three-dimensional space, making it ideal for tasks that require dexterity and accuracy. The values of the arm parameters are shown in Table I.

TABLE I. The Arm Parameter Values

| | | |
|---|---|---|
| Length of the first link | $a_1$ | 0.3m |
| Length of the second link | $a_2$ | 0.3m |
| Length of the third link | $a_3$ | 0.3m |
| Mass of the first link | $m_1$ | 2kg |
| Mass of the second link | $m_2$ | 1kg |
| Mass of the third link | $m_3$ | 1kg |

The Euler-Lagrange Formulation is the standard and basic method for obtaining the second-order dynamic equations of the studied robotic arm, where the Lagrange equation is expressed as the difference between the total kinetic energy ($Ki$) and the total potential energy ($Pi$) of each joint of the robot. This approach enables an accurate and systematic representation of the robot's dynamic behaviour, accounting for the interplay of inertia, gravity, and joint interactions. The equation of the Lagrange function is given as follows:

After obtaining Lagrange's equation, the equations of the moments acting on the rotary joints can be obtained as follows:

$$L = \sum_{0}^{3} K_i - \sum_{0}^{3} P_i \tag{1}$$

$$\tau_i = \frac{d}{dt}\frac{\partial L}{\partial \dot{\theta}_i} - \frac{\partial L}{\partial \theta_i}, i = 1,2,3 \tag{2}$$

$T_i$ is the torque acting on joint $i$, $\theta_i$ is the angle of joint $i$, $\dot{\theta}_i$ is the angular velocity of joint $i$.

The general dynamic equation for robotic arms with n-DOF rotary joints is given as:

$$\tau = M(\theta)\ddot{\theta} + V(\theta, \dot{\theta}) + G(\theta) \tag{3}$$

In the above equation, $M$ represents the inertia matrix, while the matrix $V$ includes both the carioles and centrifugal forces and finally, the matrix $G$ represents the Earth's gravity.

For the considered robotic arm with three rotary joints, the matrices $M$, $V$, and $G$ are given as (4)-(13):

$$M = \begin{bmatrix} M_{11} & 0 & 0 \\ 0 & M_{22} & M_{23} \\ 0 & M_{32} & M_{33} \end{bmatrix} \tag{4}$$

$$\begin{aligned} M_{11} = {} & 0.5m_1a_1^2 + 0.5m_1a_2^2 \\ & + m_3(a_2^2 cos\theta_2^2 \\ & + 1/3a_3^2\, cos(\theta_2 + \theta_3)^2 \\ & + a_2a_3\, cos(\theta_2 + \theta_3)\, cos\,\theta_2) \\ & + 1/3m_2a_2^2\, cos\theta_2^2 \end{aligned} \tag{5}$$

$$\begin{aligned} M_{22} = {} & 1/3\; a_2^2m_2 + a_2^2m_3 + 1/3a_3^2m_3 \\ & + a_2a_3m_3\, cos\,\theta_3 \end{aligned} \tag{6}$$

$$\begin{aligned} M_{23} = M_{32} = {} & 1/3\; a_3^2m_3 + a_2^2m_3 \\ & + 1/3a_2a_3m_3\, cos\,\theta_3 \end{aligned} \tag{7}$$

$$M_{33} = 1/3\; a_3^2m_3 \tag{8}$$

$$V(\theta, \dot{\theta}) = \begin{bmatrix} V_1 \\ V_2 \\ V_3 \end{bmatrix} \tag{9}$$

$$\begin{aligned} V_1 = {} & [-4/3\, m_2a_2^2\, sin\, 2\theta_2 \\ & - 1/3\, m_3a_3^2\, sin\, 2(\theta_2 + \theta_3) \\ & - m_3a_2a_3\, sin(2\theta_2 + \theta_3)]\dot{\theta}_1\dot{\theta}_2 \\ & + [-1/3\, m_3a_3^2\, sin\, 2(\theta_2 + \theta_3) \\ & - m_3a_2a_3\, cos\,\theta_2\, sin(\theta_2 \\ & + \theta_3)]\dot{\theta}_1\dot{\theta}_3 \end{aligned} \tag{10}$$

$$\begin{aligned} V_2 = {} & [-m_3a_2a_3\, sin\,\theta_3]\dot{\theta}_2\dot{\theta}_3 \\ & + [-0.5a_2a_3\, sin\,\theta_3]\dot{\theta}_3^{\,2} \\ & + \Big[\frac{1}{6}m_2a_2^2\, sin\, 2\theta_2 \\ & + \frac{1}{6}m_3a_3^2\, sin\, 2(\theta_2 + \theta_3) \\ & + 0.5m_3a_2^2\, sin\, 2\theta_2 \\ & + 0.5m_3a_2a_3\, sin(2\theta_2 \\ & + \theta_3)\Big]\dot{\theta}_1^{\,2} \end{aligned} \tag{11}$$

$$\begin{aligned} V_3 = {} & [0.5m_3a_2a_3\, sin\,\theta_3]\dot{\theta}_2^2 \\ & + [1/6\, m_3a_3^2\, sin\, 2(\theta_2 + \theta_3) \\ & + 0.5m_3a_2a_3\, cos\,\theta_2\, sin(2\theta_2 \\ & + \theta_3)]\dot{\theta}_1^{\,2} \end{aligned} \tag{12}$$

$$G(\theta) = \begin{bmatrix} 0 \\ 0.5m_3ga_3\, cos(\theta_2 + \theta_3) + 0.5m_2ga_2\, cos\,\theta_2 + m_3ga_2\, cos\,\theta_2 \\ 0.5m_3ga_3\, cos(\theta_2 + \theta_3) \end{bmatrix} \tag{13}$$

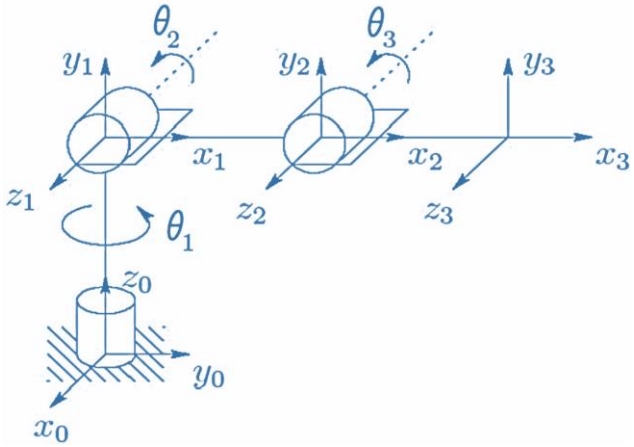


Fig. 1. The 3dof robotic arm [66], [70]

### A. The System's Linear Model

To obtain the linear model of the robotic arm, some approximations such as (14) will be made.

$$cos(x) = 1, sin(x) = 0 \tag{14}$$

By substituting (14) in the equations (8)-(15) and substituting them in the equation (3), the following is obtained:

$$\begin{bmatrix}\tau_1\\ \tau_2\\ \tau_3\end{bmatrix} = \begin{bmatrix}m_{11} & 0 & 0\\ 0 & m_{22} & m_{23}\\ 0 & m_{32} & m_{33}\end{bmatrix}\begin{bmatrix}\ddot{\theta}_1\\ \ddot{\theta}_2\\ \ddot{\theta}_3\end{bmatrix} + \begin{bmatrix}0\\ 0.5m_3ga_3 + 0.5m_2ga_2 + m_3ga_2\\ 0.5m_3ga_3\end{bmatrix} \tag{15}$$

Where:

$$m_{11} = 0.5m_1a_1^2 + 0.5m_1a_2^2 + m_3(a_2^2 + 1/3a_3^2 + a_2a_3) + 1/3m_2a_2^2$$

$$m_{22} = 1/3\ a_2^2m_2 + a_2^2m_3 + 1/3a_3^2m_3 + a_2a_3m_3$$

$$m_{23} = M_{32} = 1/3\ a_3^2m_3 + a_2^2m_3 + 1/3a_2a_3m_3$$

$$m_{33} = 1/3\ a_3^2m_3$$

After substituting the parameters listed in Table I, the linear model containing three input signals (the three torques transmitted to the joints) and six state variables (the three joint angles and the angular velocities) can be rewritten in the state space formally as follows after negotiating the G:

$$\begin{bmatrix}\dot{\theta}_1\\ \dot{\theta}_2\\ \dot{\theta}_3\\ \dot{w}_1\\ \dot{w}_2\\ \dot{w}_3\end{bmatrix} = \begin{bmatrix}0&0&0&1&0&0\\ 0&0&0&0&1&0\\ 0&0&0&0&0&1\\ 0&0&0&0&0&0\\ 0&0&0&0&0&0\\ 0&0&0&0&0&0\end{bmatrix}\begin{bmatrix}\theta_1\\ \theta_2\\ \theta_3\\ w_1\\ w_2\\ w_3\end{bmatrix} + \begin{bmatrix}0&0&0\\ 0&0&0\\ 0&0&0\\ 2.38&0&0\\ 0&-0.24&2.94\\ 0&2.94&-1.96\end{bmatrix}\begin{bmatrix}\tau_1\\ \tau_2\\ \tau_3\end{bmatrix} \tag{16}$$

## III. MIMO System Control of The Arm Robot

It is noted in relation (18) that the matrix B of the system includes a link between the input signals, to build a controller system capable of dealing with SISO systems, so a transformation matrix must be added so that the input of this matrix is the output signals of the three SISO controllers that will be placed to regulate the three positions of the joints while the output of this matrix is the three torque signals affecting the joints. This matrix is calculated as follows:

If it is assumed that we have three control signals (ua, ub, uc) representing the output of the three controllers and that the system has become of the SISO type, then relation (16) can be fixed so that it is written as (17):

$$\begin{bmatrix}\dot{\theta}_1\\ \dot{\theta}_2\\ \dot{\theta}_3\\ \dot{w}_1\\ \dot{w}_2\\ \dot{w}_3\end{bmatrix} = \begin{bmatrix}0&0&0&1&0&0\\ 0&0&0&0&1&0\\ 0&0&0&0&0&1\\ 0&0&0&0&0&0\\ 0&0&0&0&0&0\\ 0&0&0&0&0&0\end{bmatrix}\begin{bmatrix}\theta_1\\ \theta_2\\ \theta_3\\ w_1\\ w_2\\ w_3\end{bmatrix} + \begin{bmatrix}0&0&0\\ 0&0&0\\ 0&0&0\\ 1&0&0\\ 0&1&0\\ 0&0&1\end{bmatrix}\begin{bmatrix}u_a\\ u_b\\ u_c\end{bmatrix} \tag{17}$$

By matching relations (16) and (17), we find:

$$\begin{bmatrix}u_a\\ u_b\\ u_c\end{bmatrix} = \begin{bmatrix}2.38&0&0\\ 0&-0.24&2.94\\ 0&2.94&-1.96\end{bmatrix}\begin{bmatrix}\tau_1\\ \tau_2\\ \tau_3\end{bmatrix} \tag{18}$$

Thus, the transformation matrix required to calculate the required torques of the actuators can now be easily obtained from the control signals generated by the SISO controllers as follows:

$$\tau_1 = 0.42u_a \tag{19}$$

$$\tau_2 = 0.24u_b + 0.36u_c \tag{20}$$

$$\tau_3 = 0.36u_b + 0.029u_c \tag{21}$$

### A. PIDC of the Arm Robot

Considering the relationships (19) - (21). It is noted that the torque of the second and third motors is impacted by the control signal that governs the movement of the second joint, and the torque of the second and third motors is impacted by the control signal that governs the movement of the third joint. Thus, it is possible to say that the control system has evolved into a SISO-based MIMO system. Fig. 2 shows the block diagram of the MIMO control system based on PIDC.

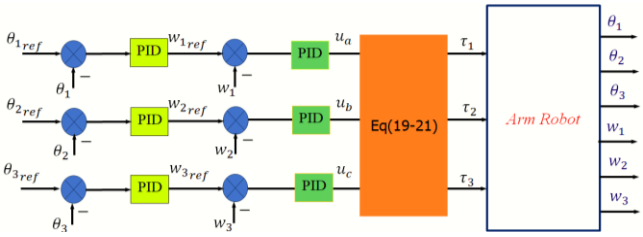


Fig. 2. Block diagram of the MIMO control system of the arm robot based on PIDC

### B. SMC of the Arm robot

SMC is a robust control method that works well in dynamic or unpredictable contexts because it can tolerate system uncertainties, parameter fluctuations, and external disturbances. Using a sliding surface that is specifically made to depict the intended system behaviour is the fundamental concept of SMC. Consistent and dependable performance results from the controller making sure that the system states converge to and stay on this surface. The system maintains stability and meets the intended control goals after it reaches the sliding surface, when it becomes essentially insensitive to uncertainties and disturbances [71]-[75].

For the state space described by the relation (17), the following relation can be written expressing the relationship between the state variable and the control signal:

$$\dot{x} = u \tag{22}$$

To make the state variable $x$ track the reference value, the sliding surface function can be written as (23):

$$S = x_{ref} - x \tag{23}$$

By deriving the equation (23), we get

$$\dot{S} = \dot{x_{ref}} - u \tag{24}$$

To attract the state variable $x$ to the sliding surface, the switching law can be written as:

$$\dot{S} = -kSgn(S) - qS \tag{25}$$

The constants $k$ presents the switching gain, and $q$ presents the proportional term.

By substituting relation (25) into relation (24), the control law for the regulation $x$ can be obtained as:

$$u = \dot{x_{ref}} + kSgn(S) + qS \tag{26}$$

For a Lyapunov function according to the relation:

$$V = 0.5S^2 \tag{27}$$

For the system to be stable, it must be achieved:

$$\dot{V} = \dot{S}S < 0 \tag{28}$$

By substitution the switching law from (25), we find:

$$\dot{V} = -kSgn(S)S - qS^2 \tag{29}$$

This confirms the necessity for the constants $k$ and $q$ to be positive values.

### C. SMC Laws of Arm Robot

By applying the methodology in section 3-2, the control laws for regulating the angular positions of the robot are obtained as in (30)-(32) and the control laws for regulating the angular velocities as in (33)-(35) after taking the relations (19)-(21) into account.

$$w_{1ref} = (\dot{\theta_{1ref}} + b_1 Sgn(\theta_{1ref} - \theta_1) + b_2(\theta_{1ref} - \theta_1) \tag{30}$$

$$w_{2ref} = (\dot{\theta_{2ref}} + b_3 Sgn(\theta_{2ref} - \theta_2) + b_4(\theta_{2ref} - \theta_2) \tag{31}$$

$$w_{3ref} = (\dot{\theta_{3ref}} + b_5 Sgn(\theta_{3ref} - \theta_3) + b_6(\theta_{3ref} - \theta_3) \tag{32}$$

$$\tau_1 = 0.4(\dot{w_{1ref}} + b_7 Sgn(w_{1ref} - w_1) + b_8(w_{1ref} - w_1)) \tag{33}$$

$$\tau_2 = 0.24(\dot{w_{2ref}} + b_9 Sgn(w_{2ref} - w_2) + b_{10}(w_{2ref} - w_2)) + 0.36(\dot{w_{3ref}} + b_{11} Sgn(w_{3ref} - w_3) + b_{12}(w_{3ref} - w_3)) \tag{34}$$

$$\tau_3 = 0.36(\dot{w_{2ref}} + b_9 Sgn(w_{2ref} - w_2) + b_{10}(w_{2ref} - w_2)) + 0.029(\dot{w_{3ref}} + b_{11} Sgn(w_{3ref} - w_3) + b_{12}(w_{3ref} - w_3)) \tag{35}$$

The constants $(b_1, b_3, b_5, b_7, b_9, b_{11})$ in the derivation of the control laws in SMC correspond to the constant k in (26). A higher value of them speeds up the convergence but may cause vibrations. The constants $(b_2, b_4, b_6, b_8, b_{10}, b_{12})$ correspond to the constant $q$ in (26). A higher value enhances stability but may cause saturation of the transient control signal and drift away from the slip surface. Experimental analysis or simulation should be performed to choose the best balance between $(b_1, b_3, b_5, b_7, b_9, b_{11})$ and $(b_2, b_4, b_6, b_8, b_{10}, b_{12})$ to achieve a fast response without excessive vibrations. Fig. 3 shows the block diagram of robot control using the sliding mode methodology.

### D. ADRC of the Arm Robot

To estimate and correct for disturbances and uncertainties in the models, a contemporary control technique called Active Disturbance Rejection Control (ADRC) has been created. The Extended State Observer (ESO), which forms the basis of ADRC, continuously monitors the system to estimate its states and the total disturbances affecting it. The control law created using these estimates dynamically adjusts the system's behaviour to compensate for the uncertainty and disturbances. Among the improvements that this controller brings are the elimination of vibrations resulting from the use of the sliding pattern methodology and the smoothing of the transient and steady state of the system, which contributes to improving the stability and performance of the robot's three-link control system [76]-[78].

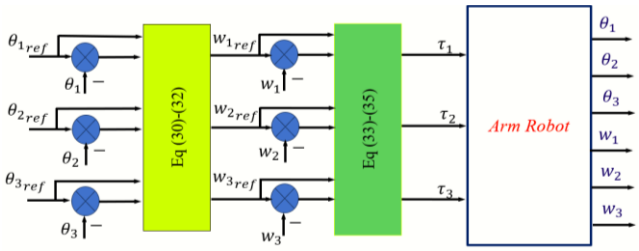


Fig. 3. The block diagram of robot system control using the sliding mode methodology

The two primary parts of a LADRC are an ESO and a proportional controller (kp) as shown in Fig. 4(a). To enable the controller to actively correct for these impacts, the ESO is in charge of calculating the generalized disturbance as well as the system states. The tracking error is used by the proportional controller to drive the error to zero, guaranteeing precise and consistent tracking performance [79], [80].

To regulate the angular position for one joint of the arm using an ADRC, the state space is defined as follows:

$$\frac{d\theta_{(t)}}{dt} = f(\theta, d, t) + b_0 u_{(t)} \quad i = 1,2,3 \tag{36}$$

Where $f(\theta, d, t)$ is the dynamical model and any internal or external system disturbances, and b0 is the known parameter of the system. $u_{(t)}$ is the control input which represents the reference angular velocity $w_{ref}$. Equation (36) can be transformed into a state-space representation for better control and observer design as follows:

$$\frac{dz_1}{dt} = z_2 + b_0 u_{(t)} \tag{37}$$

$$\frac{dz_2}{dt} = \frac{df}{dt} \tag{38}$$

Where, $z_1$ is the Represents the system's output ($\theta$). $z_2$ is the Represents the dynamics of any internal or external system disturbances like the effect of the angular velocity regulation loop using SMC which is the inner loop of the control system.

To estimate the system states $z_1$ and $z_2$, the observer equations are given as follows:

$$\frac{dz_1}{dt} = z_2 + b_0 u_{(t)} - B_1 e \tag{39}$$

$$\frac{dz_2}{dt} = -B_2 e \tag{40}$$

$$e = z_1 - \theta \tag{41}$$

Where $[B_1\ B_2] = [2\omega_0\ \omega_0^2]$ is the observer gain vector. $\omega_0$ denotes the observer's cut-off pulse,

The control input $u_{(t)}$ is formulated as:

$$u_{(t)} = \frac{u_o - z_2}{b_0} \tag{42}$$

Where $u_o$ is defined as:

$$u_0 = k_p(r - z_1) \tag{43}$$

The controller gain $k_p$ is denoted $\omega c$, which is the closed loop natural frequency and $r$ is the reference signal. Fig. 4(b) shows the block diagram of the proposed control system.

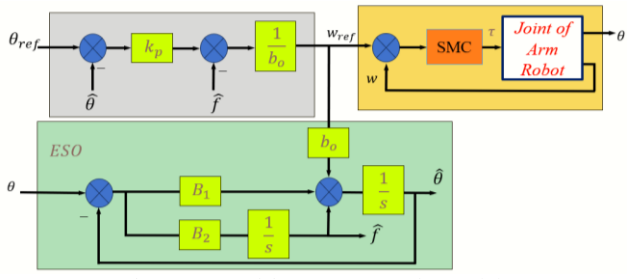


a. The Structure of the ADRC-SMC for one joint

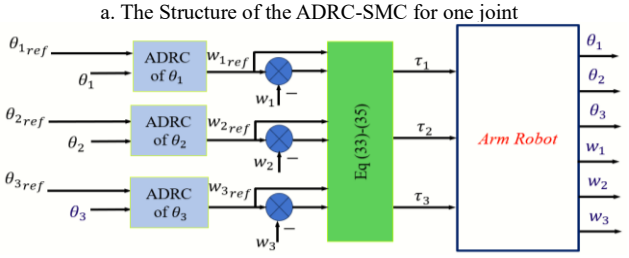


b. The Structure of the ADRC-SMC of the arm's angular positions

Fig. 4. The Structure of the ADRC-SMC

### *E. Observer and Dynamics of ADRC*

1. To account for all system uncertainties and disturbances, the observer estimates $z_1$ (output) and $z_2$ (generalized disturbance). Fast estimation is possible with a large observer gain ($\omega_0$), although noise amplification is more likely.
2. The proportional controller drives the tracking error to zero by ensuring that the system output $z_1$ tracks the reference signal.
3. To guarantee precise state estimates, the observer needs to be quicker than the controller. The observer's poles ($\omega_0$) are positioned to the left of the controller poles ($k_p$) to do this. $\omega_0$ is usually selected as $\omega_0 = (3 - 10)\, k_p$ [79], [80].

Fig. 5 shows the bode plot characteristics of the open loop control system of angular positions of the arm, for different values of $\omega_0$, where $b0 = 1\ and\ kp = 222$.

It can be seen that with increasing the value of $\omega_0$, the system's response is faster, but it becomes less robust and stable, so an intermediate value can be taken that ensures the stability and robustness of the system while maintaining fast-tracking of the reference signal.

## IV. SIMULATION RESULTS

The main goal of robot control is to adjust the operating torque in such a way that it follows the desired path as accurately as possible, and as quickly as possible. To test the effectiveness of the proposed control system, a simulation was performed in a MATLAB/Simulink environment to track a circular path. Fig. 6, Fig. 7, and Fig. 8 show the tracking response for the first, second, and third joints, respectively.

It is clear from Fig. 6, Fig. 7, Fig. 8 that the performance of the proposed ADRC-SMC control system is superior, as it achieves higher tracking accuracy and no vibration.

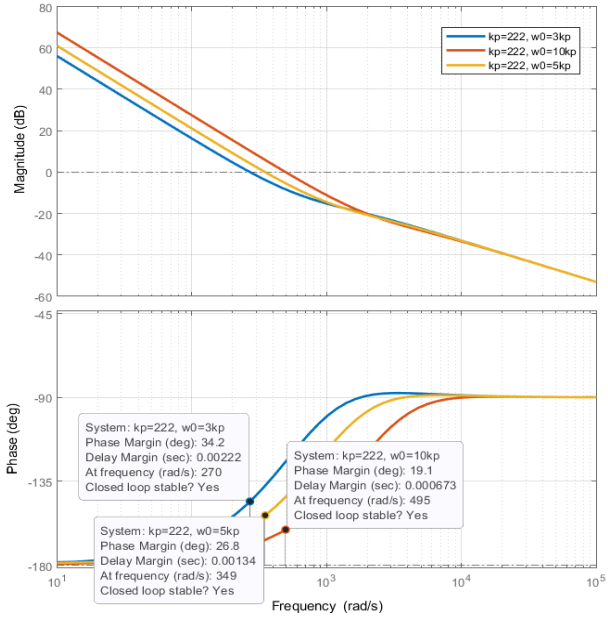


Fig. 5. The bode plot characteristics of the open loop control system of the position

By examining Fig. 6, it is noted that the PID-based control system has the advantage of less vibration than the sliding mode control system, while the sliding mode control system is more effective in tracking speed when there is a change in the reference signal. The same can be noted in Fig. 7 where it is noted that the joint deviates from the desired path at the moment of starting operation, then returns to the desired path, and the same can be noted at moment 6.5 sec. The proposed ADRC-SM control system combines the advantages of both control systems (PID and SM) as it is more effective in tracking accuracy and speed with a clear reduction in vibrations caused by the control system based only on the sliding mode. This can be verified by examining Fig. 8 when tracking a fixed-value reference.

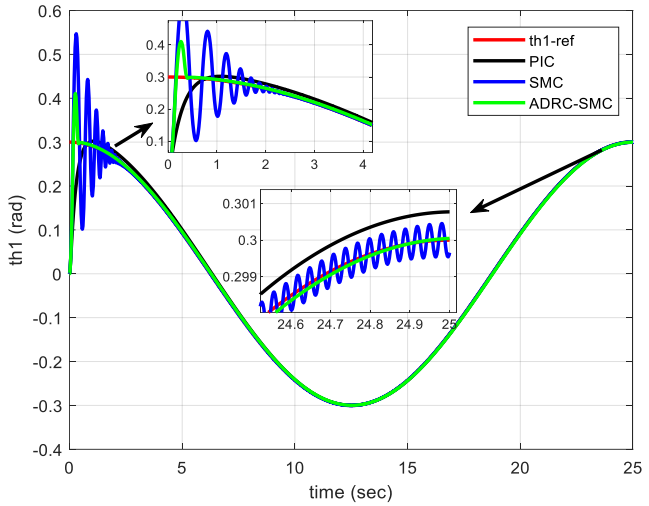


Fig. 6. The tracking response for the first joint

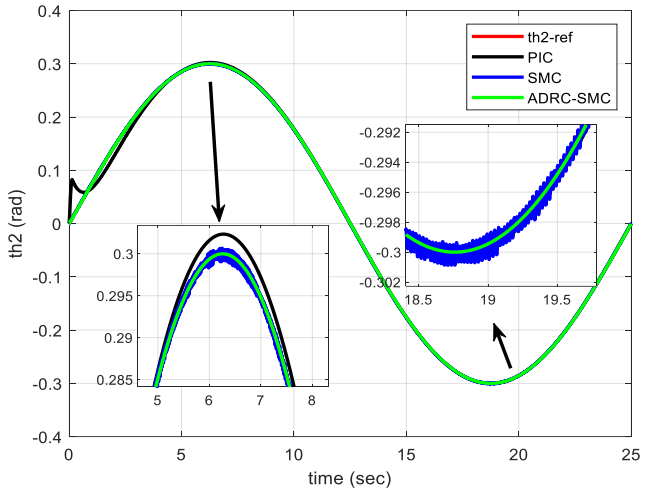


Fig. 7. The tracking response for the second joint

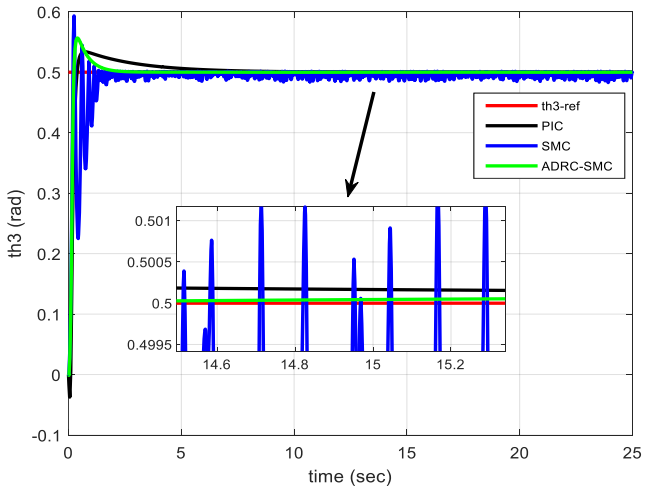


Fig. 8. The tracking response for the third joint

By examining Fig. 6, it is noted that the PID-based control system has the advantage of less vibration than the sliding mode control system, while the sliding mode control system is more effective in tracking when a change in the reference signal occurs. The same can be observed in Fig. 7, where it is noted that the joint deviates from the desired path at the starting moment, then return to it and maintains good tracking, and the same can be observed at the moment 6.5 sec. However, when using the proposed control system, both advantages can be obtained. Examining Fig. 8 shows that the PID-based control system is superior compared to the sliding mode control system as no significant vibrations occur, but it has a longer settling time, while the proposed ADRC-SM control system combines the advantages of the two control systems (PIDC-SMC) as it is more effective in tracking accuracy and faster with a clear reduction in vibrations resulting from the sliding mode-based control system only.

Fig. 9 shows a comparison between the error average values for tracking the reference signals of the joints using the three control systems presented in this research. It is noted that the proposed control system achieves the lowest error average. The tracking error average value of the first joint is 0.0035 rad using ADRC-SMC, 0.006 rad using PIDC, and 0.007 rad using SMC. For the second joint, it is noted that the average tracking error value is 0.0004 rad using ADRC-SMC, 0.00044 rad using SMC, and 0.0033 rad using PIDC. For the third joint, it is noted that the average tracking error value is 0.0044 rad using ADRC-SMC, 0.0077 rad using PIDC, and 0.012 rad using SMC.

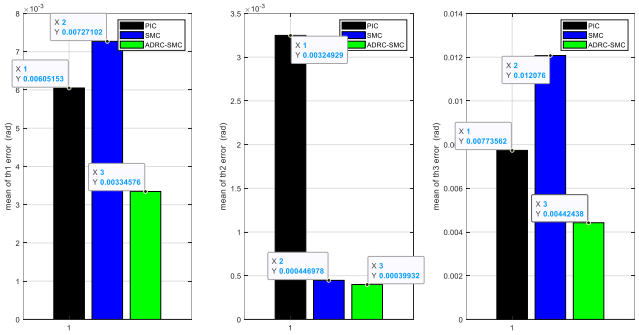


Fig. 9. A comparison between the error average values for tracking the reference signals of the joints

The control signals applied to the three motors are shown in Fig. 10, Fig. 11 and Fig. 12, and it is clear that the proposed control system (ADRC-SMC) outperforms the SMC system in its effectiveness in generating a smooth and vibration-free control signal. On the other hand, a difference is observed between the torque values required to rotate the three joints of the arm, which can be explained by referring to equation (15). It is noted from Fig. 10 that the torque required for the first joint is low compared to the second and third joints, as the first joint is supported on the base and the first joint forms a right angle with the ground, which means that the gravitational force acting on it is zero. It is noted from Fig. 11 that the torque required to rotate the second joint is greater compared to the first and second joints, as the second joint carries both the second and third joints, which means that the torque required to overcome the gravitational force is greater. It is noted from Fig. 12 that the torque required to rotate the third joint is less compared to the torque of the second joint because the effect of the gravitational force is less, as shown in equation (15).

To test the time-responses characteristics of control systems, a test was conducted to track reference signals with a constant value (step response, $ref = 0.1\,rad$). Fig. 13

shows the response of the first joint, Fig. 14 shows the response of the second joint, and Fig. 15 shows the response of the third joint.

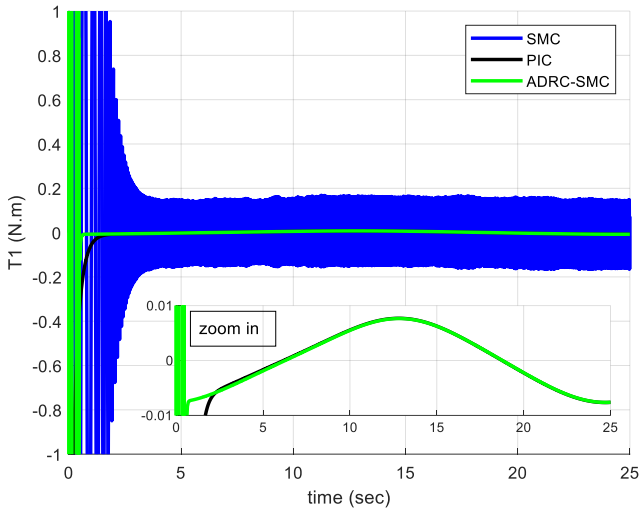


Fig. 10. The control signal applied to the first actuator

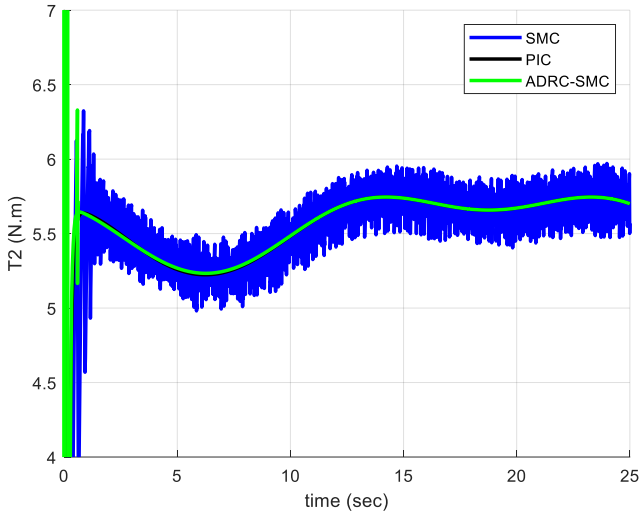


Fig. 11. The control signal applied to the second actuator

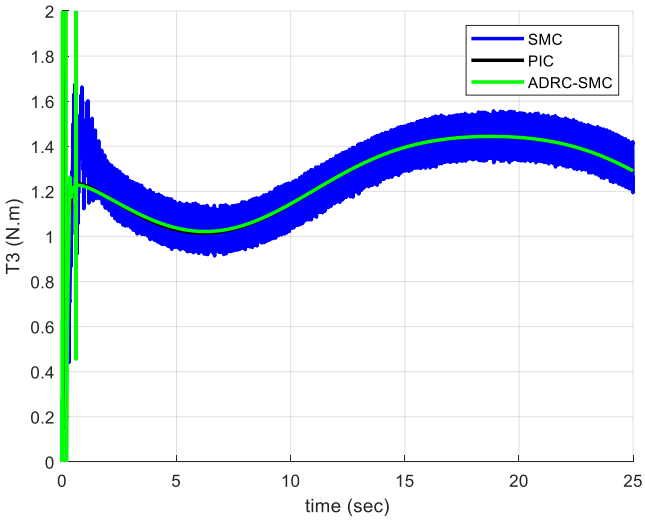


Fig. 12. The control signal applied to the third actuator

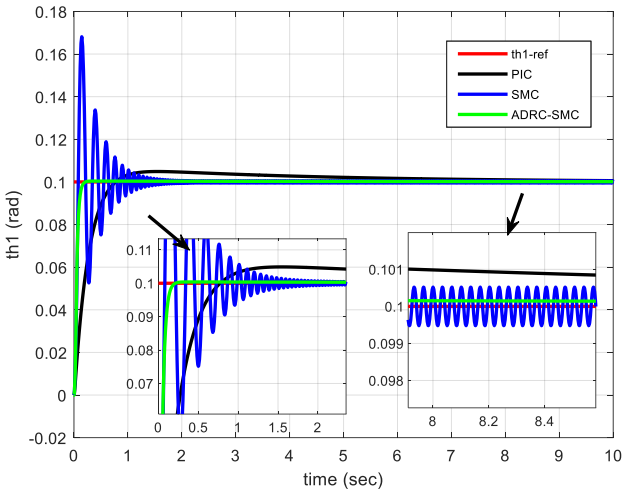


Fig. 13. The response of the first joint for step response, $ref = 0.1\ rad$

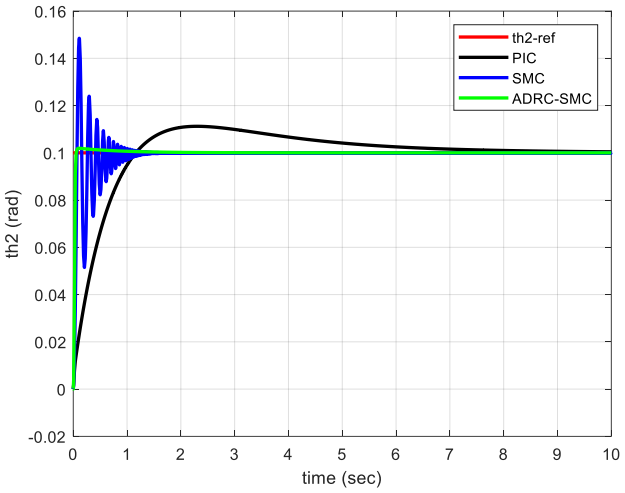


Fig. 14. The response of the second joint step response, $ref = 0.1\ rad$

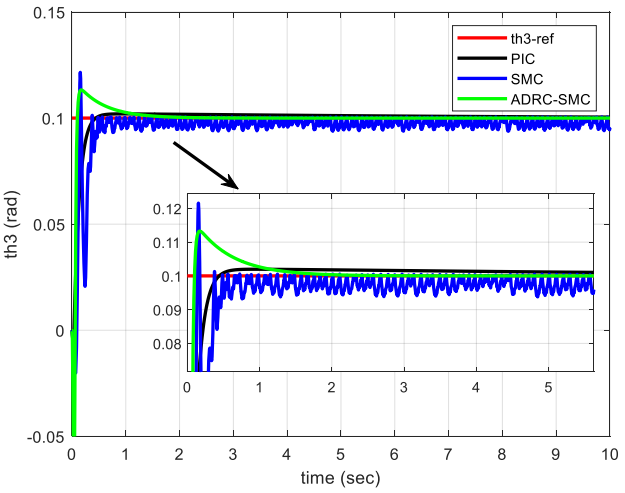


Fig. 15. The response of the third joint step response, $ref = 0.1\ rad$

It is noted from the Fig. 13 that the proposed control system achieves better performance in terms of tracking fast and accuracy, the settling time is 0.02 sec, while it is noted that the settling time using the SM controller is 1.7 sec, followed by the PID control system where the settling time reaches 5.2 secs. The overshoot using the proposed controller

is zero, while it is 4% using the PID control system and 70% using the SM controller. For the second joint, it is also noted from Fig. 14 that the proposed control system achieves better performance in terms of tracking fast and accuracy, the settling time is 0.01 sec, while it is noted that the settling time using the SM controller is 0.5 sec, followed by the PID control system where the settling time reaches 6.2 secs. The overshoot using the proposed controller is zero, while it is 10% using the PID control system and 40% using the SM controller. As can be seen from Fig. 15, the proposed control system achieves the best performance in terms of tracking accuracy and achieving a lower static error.

The reasons for the superiority of the ADRC-SMC control system can be summarized as follows:

1) The use of ADRC in the external control loop provides a proactive estimation and monitoring mechanism to compensate for disturbances and uncertainties in the system, making it able to generate a control signal for the internal loop faster without the need for a long damping period. This allows the internal SMC loop to respond faster, which significantly reduces the settling time.
2) Also, the presence of a disturbance monitor contributes to achieving more precise control of the system response, preventing large overshoots as in PID or even SMC.
3) Unlike PID, which can introduce overshoot due to its integral action, ADRC-SMC dynamically adjusts the control effort, ensuring a smoother and more precise response.
4) The use of SMC in the internal control loop contributes to achieving system robustness and increasing response speed; SMC ensures high robustness against parameter variations and disturbances, while ADRC enhances adaptability, achieving optimal performance.

Regarding the limits of this system or its degree of complexity, by looking at Fig. 4(a), we notice that the degree of complexity of the control system ADRC is not very large compared to traditional control systems, as it includes a proportional limit in the control law, while the disturbance monitor includes a proportional limit in addition to two complementary limits.

## V. CONCLUSION

This study deals with the design and evaluation of a hybrid control system that combines sliding control (SMC) and active disturbance cancellation (ADRC) to improve the response of a 3-DoF robotic arm. By utilising the robustness of classic SMC, the proposed sys tem sought to minimise its inherent vibrations while guarant eeing smooth, quick, and extremely dynamic responses with efficient disturbance rejection.

Different scenarios were conducted in the simulation environment to track a circular path, as well as to track fixed-value reference signals for the three joints. Table II shows a summary of the simulation results including a comparison of the performance of control systems during circular trajectory tracking and when regulating angular positions at fixed values.

The results in Table II show that the classical SMC control methodology provides superior performance compared to the traditional PIDC from the low stability time, but suffers from a higher value of path tracking error as well as a higher value of target overshoot. In contrast, the proposed control methodology contributes to improving the performance of the robotic arm, achieving faster response, lower value of target overshoot as well as lower value of path tracking error.

To provide a clear evaluation of the performance, Table III compares the PIDC, SMC and ADRC-SMC control methods based on the main performance criteria.

From the above comparison, it is clear that the ADRC-SMC controller outperforms both PIDC and SMC by providing superior tracking accuracy, fast response, and significantly reduced vibration. This makes it a promising solution for high-precision robotics applications, especially in industrial automation, medical robotics, etc. Its ability to balance robustness, speed, and accuracy while mitigating vibrations makes it the ideal choice for controlling multi-degree-of-freedom robotic systems.

TABLE II. A SUMMARY OF THE SIMULATION RESULTS

| | | | ADRC-SMC | PIDC | SMC |
|---|---|---|---|---|---|
| **Joint 1** | Fixed reference signals | Settling Time | 0.02 (sec) | 5.2 (sec) | 1.7 (sec) |
| | | Overshoot | 0% | 4% | 70% |
| | circular reference path | tracking error average | 0.0035 rad | 0.006 rad | 0.007rad |
| **Joint 2** | Fixed reference signals | Settling Time | 0.01 sec | 6.2sec | 0.5 sec |
| | | Overshoot | 0% | 10% | 40% |
| | circular reference path | tracking error average | 0.0004 rad | 0.0033 rad | 0.00044 rad |
| **Joint 3** | Fixed reference signals | Settling Time | 0.7 sec | 0.5 sec | 0.5 sec |
| | | Overshoot | 11% | 0% | 21% |
| | circular reference path | tracking error average | 0.0044 rad | 0.0077 rad | 0.012 rad |

TABLE III. COMPARING THE PERFORMANCE OF THE CONTROL METHODS

| Performance Criterion | PIDC | SMC | ADRC-SMC (Proposed) |
|---|---|---|---|
| **Tracking Accuracy** | Good | Moderate | Excellent |
| **Settling Time** | big | small | Very small |
| **Overshoot** | Low | High | Very low |
| **Vibration Reduction** | Low | High | Nearly Eliminated |
| **Implementation Complexity** | Easy | Moderate | Relatively Complex |
| **Overall Performance** | Average | Good | Excellent |

## REFERENCES


[1] A. Ashagrie, A. O. Salau, and T. Weldcherkos, "Modelling and control of a 3-DOF articulated robotic manipulator using a self-tuning fuzzy sliding mode controller," *Cogent Engineering*, vol. 8, no. 1, p. 1950105, 2021.

[2] P. Saraf and R. N. Ponnalagu, "Modelling and simulation of a point-to-point spherical articulated manipulator using optimal control," *2021 7th International Conference on Automation, Robotics and Applications (ICARA)*, pp. 152-156, 2021.

[3] H. Xiong, R. Mendonca, K. Shaw, and D. Pathak, "Adaptive mobile manipulation for articulated objects in the open world," *arXiv*, 2024.

[4] M. Tomar, S. Mandava, N. Hemalatha, V. R. Rao, and R. K. Mandava, "Design of PID, FLC and Sliding Mode Controller for 2-DOF Robotic Manipulator: A Comparative Study," *International Journal of Mathematical, Engineering and Management Sciences*, vol. 8, no. 1, p. 94, 2023.

[5] K. Khalid, A. A. Zaidi, and Y. Ayaz, "Optimal Placement and Kinematic Design of 2-DoF Robotic Arm," *2021 International Bhurban Conference on Applied Sciences and Technologies (IBCAST)*, pp. 552-559, 2021.

[6] W. Adris Shutnan *et al*., "Modeling and Control of a 3DOF Robot Manipulator Using Artificial Fuzzy-Immune FOPID Controller," *IEEE Access*, vol. 12, pp. 153074-153088, 2024.

[7] K. M. Raheem and A. N. Najaf, "Simulation 3-DOF R Robotic Manipulator under PID Controller," *Journal of Engineering and Applied Sciences*, vol. 15, no. 2, pp. 410-414, 2020.

[8] D. H. Nguyen, V. D. Truong, and N. T. Lam, "Nonlinear control of a 3-DOF robotic arm driven by electro-pneumatic servo systems," *Measurement, Control, and Automation*, vol. 3, no. 1, pp. 51-59, 2022.

[9] M. Djennane, S. E. Chehaidia, C. Yakoub, K. Mesbah, M. Aljohani, and M. I. Mosaad, "Design, Analysis, and Implementation of a 3-DOF Spherical Parallel Manipulator," *IEEE Access*, vol. 12, pp. 52837-52850, 2024.

[10] N. G. Adar, "Real-time control application of the robotic arm using neural network-based inverse kinematics solution," *Sakarya University Journal of Science*, vol. 25, no. 3, pp. 849-857, 2021.

[11] P. Chotikunnan and R. Chotikunnan, "Dual design PID controller for robotic manipulator application," *Journal of Robotics and Control (JRC)*, vol. 4, no. 1, pp. 23-34, 2023.

[12] T. N. Truong, A. T. Vo, and H. J. Kang, "An adaptive terminal sliding mode control scheme via neural network approach for path-following control of uncertain nonlinear systems," *International Journal of Control, Automation and Systems*, vol. 20, no. 6, pp. 2081-2096, 2022.

[13] H. Zhang, H. Fang, D. Zhang, X. Luo, and Q. Zou, "Adaptive Fuzzy Sliding Mode Control for a 3-DOF Parallel Manipulator with Parameters Uncertainties," *Complexity*, vol. 2020, no. 1, p. 2565316, 2020.

[14] H. Bilal, B. Yin, M. S. Aslam, Z. Anjum, A. Rohra, and Y. Wang, "A practical study of active disturbance rejection control for a rotary flexible joint robot manipulator," *Soft Computing*, vol. 27, no. 8, pp. 4987-5001, 2023.

[15] S. Rahimi, H. Jalali, M. R. H. Yazdi, A. Kalhor, and M. T. Masouleh, "Design and practical implementation of a Neural Network self-tuned Inverse Dynamic Controller for a 3-DoF Delta parallel robot based on Arc Length Function for smooth trajectory tracking," *Mechatronics*, vol. 84, p. 102772, 2022.

[16] W. H. Zayer, A. J. F. Ali, and Z. A. Maeedi, "3DOF Robot Arm Control Using Fuzzy Neural Petri Net (FNPN) Controller," *Journal of Engineering Science and Technology*, vol. 16, no. 6, pp. 4910-4919, 2021.

[17] C. Véronneau *et al*., "Multifunctional Remotely Actuated 3-DOF Supernumerary Robotic Arm Based on Magnetorheological Clutches and Hydrostatic Transmission Lines," *IEEE Robotics and Automation Letters*, vol. 5, no. 2, pp. 2546-2553, 2020.

[18] D. T. Tran, T. N. Nguyen, M. T. Nguyen, V. T. Ngo, and H. L. Le, "Synchronous Sliding Mode Control for a 4-DOF Parallel Manipulator in Practice," *Journal of Technical Education Science*, vol. 18, no. 03, pp. 1–13, 2023.

[19] R. Patelski and P. Dutkiewicz, "On the stability of ADRC for manipulators with modelling uncertainties," *ISA Transactions*, vol. 102, pp. 295-303, 2020.

[20] Z. Liu, K. Peng, L. Han, and S. Guan, "Modeling and control of robotic manipulators based on artificial neural networks: a review," *Iranian Journal of Science and Technology, Transactions of Mechanical Engineering*, vol. 47, no. 4, pp. 1307-1347, 2023.

[21] W. A. Shatnan, M. D. H. Almawlawe, and M. A. A. A. Jabur, "Optimal Fuzzy-FOPID, Fuzzy-PID Control Schemes for Trajectory Tracking of 3DOF Robot Manipulator," *Tikrit Journal of Engineering Sciences*, vol. 30, no. 4, pp. 46-53, 2023.

[22] A. N. Wazzan, N. Basil, M. Raad, and H. K. Mohammed, "PID controller with robotic arm using an optimization algorithm," *International Journal of Mechanical Engineering*, vol. 7, no. 2, pp. 3746-3751, 2022.

[23] J. Li and W. Li, "On-Line PID Parameters Optimization Control for Wind Power Generation System Based on Genetic Algorithm," *IEEE Access*, vol. 8, pp. 137094-137100, 2020.

[24] Y. Zhou, X. He, F. Shao, and X. Zhang, "Research on the Optimization of the PID Control Method for an EOD Robotic Manipulator Using the PSO Algorithm for BP Neural Networks," *Actuators*, vol. 13, no. 10, p. 386, 2024.

[25] Y. Xu, X. Wang, Y. Zhai, C. Li, and Z. Gao, "Precise variable spraying system based on improved genetic proportional-integral-derivative control algorithm," *Transactions of the Institute of Measurement and Control*, vol. 43, no. 14, pp. 3255-3266, 2021.

[26] M. Alam, M. S. Alam, M. Roman, M. Tufail, M. U. Khan, and M. T. Khan, "Real-Time Machine-Learning Based Crop/Weed Detection and Classification for Variable-Rate Spraying in Precision Agriculture," *2020 7th International Conference on Electrical and Electronics Engineering (ICEEE)*, pp. 273-280, 2020.

[27] L. Shi, X. Miao, and H. Wang, "An improved nonlinear proportional-integral-differential controller combined with fractional operator and symbolic adaptation algorithm," *Transactions of the Institute of Measurement and Control*, vol. 42, no. 5, pp. 927-941, 2020.

[28] M. Bi, "Control of robot arm motion using trapezoid fuzzy two-degree-of-freedom PID algorithm," *Symmetry*, vol. 12, no. 4, p. 665, 2020.

[29] M. J. Mohamed, B. K. Oleiwi, A. T. Azar, and I. A. Hameed, "Coot optimization algorithm-tuned neural network-enhanced PID controllers for robust trajectory tracking of three-link rigid robot manipulator," *Heliyon*, vol. 10, no. 13, p. e32661, 2024.

[30] M. Barfi, H. Karami, F. Faridi, Z. Sohrabi, and M. Hosseini, "Improving robotic hand control via adaptive Fuzzy-PI controller using classification of EMG signals," *Heliyon*, vol. 8, no. 12, p. e11931, 2022.

[31] M. A. Basal and M. F. Ahmed, "Mathematical Modeling of a Unicycle Robot and Use of Advanced Control Methodologies for Multi-Paths Tracking Taking into Account Surface Friction Factors," *Journal of Robotics and Control (JRC)*, vol. 6, no. 1, pp. 142-154, 2025.

[32] I. E. Putro and R. A. Duhri, "Longitudinal stability augmentation control for turbojet UAV based on linear quadratic regulator (LQR) approach," *AIP Conference Proceedings*, vol. 2226, no. 1, p. 020013, 2020.

[33] J. K. Adamu, M. F. Hamza, and A. I. Isa, "Performance comparisons of hybrid fuzzy-lqr and hybrid pid-lqr controllers on stabilizing double rotary inverted pendulum," *Journal of Applied Materials and Technology*, vol. 1, no. 2, pp. 71-80, 2020.

[34] R. Murali and P. S. King, "Reinforcement Learning assisted LQR Tuning of a Load Bearing Robotic Arm," *Journal of Physics: Conference Series*, vol. 2923, no. 1, p. 012009, 2024.

[35] Z. Li, S. Li, A. Francis, and X. Luo, "A Novel Calibration System for Robot Arm via an Open Dataset and a Learning Perspective," *IEEE Transactions on Circuits and Systems II: Express Briefs*, vol. 69, no. 12, pp. 5169-5173, 2022.

[36] C. Choubey and J. Ohri, "GWO-based tuning of LQR-PID controller for a 3-DOF parallel manipulator," *IETE Journal of Research*, vol. 69, no. 7, pp. 4378-4393, 2023.

[37] M. H. Zafar, H. B. Younus, S. K. R. Moosavi, M. Mansoor, and F. Sanfilippo, "Online PID Tuning of a 3-DoF Robotic Arm Using a Metaheuristic Optimisation Algorithm: A Comparative Analysis," *International Conference on Information and Software Technologies*, pp. 25-37, 2023.

[38] B. Varma, N. Swamy, and S. Mukherjee, "Trajectory Tracking of Autonomous Vehicles using Different Control Techniques(PID vs

LQR vs MPC)," *2020 International Conference on Smart Technologies in Computing, Electrical and Electronics (ICSTCEE)*, pp. 84-89, 2020.

[39] Ç. Uyulan, "Design and stability analysis of a robust-adaptive sliding mode control applied on a robot arm with flexible links," *Vibration*, vol. 5, no. 1, pp. 1-19, 2021.

[40] A. J. Humaidi, I. K. Ibraheem, A. T. Azar, and M. E. Sadiq, "A New Adaptive Synergetic Control Design for Single Link Robot Arm Actuated by Pneumatic Muscles," *Entropy*, vol. 22, no. 7, p. 723, 2020.

[41] H. M. Tuan, F. Sanfilippo, and N. V. Hao, "A novel adaptive sliding mode controller for a 2-DOF elastic robotic arm," *Robotics*, vol. 11, no. 2, p. 47, 2022.

[42] M. T. Vo *et al*., "Back-stepping control for rotary inverted pendulum," *Journal of Technical Education Science*, vol. 15, no. 4, pp. 93-101, 2020.

[43] M. Ahmadijokani, M. Mehrasa, M. Sleiman, M. Sharifzadeh, A. Sheikholeslami, and K. Al-Haddad, "A Back-Stepping Control Method for Modular Multilevel Converters," *IEEE Transactions on Industrial Electronics*, vol. 68, no. 1, pp. 443-453, 2021.

[44] L. Ma, Y. Yan, Z. Li, and J. Liu, "A novel aerial manipulator system compensation control based on ADRC and backstepping," *Scientific Reports*, vol. 11, no. 1, p. 22324, 2021.

[45] M. J. Mahmoodabadi and N. R. Babak, "A multi-objective optimized fuzzy back-stepping controller for a nonlinear unmanned aerial vehicle," *Research Square*, 2023.

[46] I. Al-Darraji *et al*., "Adaptive robust controller design-based RBF neural network for aerial robot arm model," *Electronics*, vol. 10, no. 7, p. 831, 2021.

[47] X. Liu and H. He, "Fault Diagnosis for TE Process Using RBF Neural Network," *IEEE Access*, vol. 9, pp. 118453-118460, 2021.

[48] L. Bao, D. Kim, S. J. Yi, and J. Lee, "Design of a sliding mode controller with fuzzy rules for a 4-DoF service robot," *International Journal of Control, Automation and Systems*, vol. 19, no. 8, pp. 2869–2881, 2021.

[49] A. M. Abdul-Sadah, K. M. Raheem, and M. M. S. Altufaili, "A fuzzy logic controller for a three-link robotic manipulator," *AIP Conference Proceedings*, vol. 2386, no. 1, 2022.

[50] M. Savarese, "Simulation & Analysis of Coupled 2R Manipulator using ADRC Control," *Master's thesis, Drexel University*, 2024.

[51] F. Doostdar and H. Mojallali, "An ADRC-based backstepping control design for a class of fractional-order systems," *ISA transactions*, vol. 121, pp. 140-146, 2022.

[52] M. Tian, B. Wang, Y. Yu, Q. Dong, and D. Xu, "Discrete-Time Repetitive Control-Based ADRC for Current Loop Disturbances Suppression of PMSM Drives," *IEEE Transactions on Industrial Informatics*, vol. 18, no. 5, pp. 3138-3149, 2022.

[53] Y. Liu, Y. Chen, Y. Gong, and G. Zhao, "Research on Active Disturbance Rejection Algorithm for Loading Control of 3-DOF Parallel Robot," *Journal of Advanced Computational Intelligence and Intelligent Informatics*, vol. 27, no. 5, pp. 923-931, 2023.

[54] X. Shi, J. Huang, and F. Gao, "Fractional-Order Active Disturbance Rejection Controller for Motion Control of a Novel 6-DOF Parallel Robot," *Mathematical Problems in Engineering*, vol. 2020, no. 1, p. 3657848, 2020.

[55] X. Li, B. Liu, and L. Wang, "The control system of the six-axis serial manipulator is based on active disturbance rejection control," *International Journal of Advanced Robotic Systems*, vol. 17, no. 4, 2020.

[56] A. Eltayeb, G. Ahmed, I. H. Imran, N. M. Alyazidi, and A. Abubaker, "Comparative analysis: Fractional PID vs. PID controllers for robotic arm using genetic algorithm optimization," *Automation*, vol. 5, no. 3, pp. 230-245, 2024.

[57] S. Husnain and R. Abdulkader, "Fractional Order Modeling and Control of an Articulated Robotic Arm," *Engineering, Technology & Applied Science Research*, vol. 13, no. 6, pp. 12026-12032, 2023.

[58] R. D. Xi, T. N. Ma, X. Xiao, and Z. X. Yang, "Design and implementation of an adaptive neural network observer-based backstepping sliding mode controller for robot manipulators," *Transactions of the Institute of Measurement and Control*, vol. 46, no. 6, pp. 1093-1104, 2024.

[59] H. Wu *et al*., "Parallel network-based sliding mode tracking control for robotic manipulators with uncertain dynamics," *Actuators*, vol. 12, no. 5, p. 187, 2023.

[60] K. Huang and Z. Wang, "Research on robust fuzzy logic sliding mode control of Two-DOF intelligent underwater manipulators," *Mathematical Biosciences and Engineering (MBE)*, vol. 20, no. 9, pp. 16279-16303, 2023.

[61] P. Saraf and R. N. Ponnalagu, "Modeling and Simulation of a Point to Point Spherical Articulated Manipulator Using Optimal Control," *2021 7th International Conference on Automation, Robotics and Applications (ICARA)*, pp. 152-156, 2021.

[62] P. Gümbel, X. He, and K. Dröder, "Precision optimized pose and trajectory planning for vertically articulated robot arms," *Procedia CIRP*, vol. 106, pp. 185-190, 2022.

[63] M. Mohamed, F. Anayi, M. Packianather, B. A. Samad, and K. Yahya, "Simulating LQR and PID controllers to stabilise a three-link robotic system," *2022 2nd International Conference on Advance Computing and Innovative Technologies in Engineering (ICACITE)*, pp. 2033-2036, 2022.

[64] K. S. K. Suryanarayana, "Adaptive LQR-based Control of 3-DOF Spherical Articulated Robotic Manipulator," *Research Square*, 2024.

[65] M. K. Jangid, S. Kumar, and J. Singh, "Trajectory tracking optimization and control of a three-link robotic manipulator for application in casting," *International Journal of Advanced Technology and Engineering Exploration*, vol. 8, no. 83, p. 1255, 2021.

[66] S. Vtyurina and D. Shilin, "Calculation, modeling and programming of a three-link manipulator robot," *2023 5th International Youth Conference on Radio Electronics, Electrical and Power Engineering (REEPE)*, pp. 1-6, 2023.

[67] A. N. Sharkawy and S. S. Khairullah, "Forward and Inverse Kinematics Solution of A 3-DOF Articulated Robotic Manipulator Using Artificial Neural Network," *International Journal of Robotics & Control Systems*, vol. 3, no. 2, pp. 330-353, 2023.

[68] C. E. Agbaraji, U. H. Udeani, H. C. Inyiama, and C. C. Okezie, "Robust Control for a 3DOF Articulated Robotic Manipulator Joint Torque under Uncertainties," *Journal of Engineering Research and Reports*, vol. 9, no. 4, pp. 1-13, 2020.

[69] S. V. Alekseeva, V. A. Sokolova, and V. A. Markov, "Mathematical modelling of one type of three-link robot manipulator," *IOP Conference Series: Earth and Environmental Science*, vol. 421, no. 4, p. 042005, 2020.

[70] M. I. Azeez, A. M. M. Abdelhaleem, S. Elnaggar, K. A. Moustafa, and K. R. Atia, "Optimized sliding mode controller for trajectory tracking of flexible joints three-link manipulator with noise in input and output," *Scientific Reports*, vol. 13, no. 1, p. 12518, 2023.

[71] C. J. Lin, T. Y. Sie, W. L. Chu, H. T. Yau, and C. H. Ding, "Tracking control of pneumatic artificial muscle-activated robot arm based on sliding-mode control," *Actuators*, vol. 10, no. 3, p. 66, 2021.

[72] Y. Xu, R. Liu, J. Liu, and J. Zhang, "A novel constraint tracking control with sliding mode control for industrial robots," *International Journal of Advanced Robotic Systems*, vol. 18, no. 4, 2021.

[73] T. Kamel, D. Abdelkader, B. Said, and A. Iqbal, "Sliding mode control of grid-connected wind energy system driven by 2 five-phase permanent magnet synchronous generators controlled by a new fifteen-switch converter," *International Transactions on Electrical Energy Systems*, vol. 30, no. 9, p. e12480, 2020.

[74] A. M. Osman and F. Alsokhiry, "Sliding Mode Control for Grid Integration of Wind Power System Based on Direct Drive PMSG," *IEEE Access*, vol. 10, pp. 26567-26579, 2022.

[75] J. Wang, Q. Miao, X. Zhou, L. Sun, D. Gao, and H. Lu, "Current Control Method of Vehicle Permanent Magnet Synchronous Motor Based on Active Disturbance Rejection Control," *World Electric Vehicle Journal*, vol. 14, no. 1, p. 2, 2022.

[76] H. Hu, S. Xiao, and H. Shen, "Modified linear active disturbance rejection control for uncertain robot manipulator trajectory tracking," *Mathematical Problems in Engineering*, vol. 2021, no. 1, pp. 1-13, 2021.

[77] X. Zhou, J. Wang, and Y. Ma, "Linear active disturbance rejection control of grid-connected photovoltaic inverter based on deviation control principle," *Energies*, vol. 13, no. 15, p. 3790, 2020.

[78] C. Cheng *et al*., H. Zhang, H. Peng, Z. Zhou, B. Chen, Z. Zeng, and H. Lu, "Stability control for end effect of mobile manipulator in uneven terrain based on active disturbance rejection control," *Assembly Automation*, vol. 41, no. 3, pp. 369–383, 2021.

[79] Y. Zeng *et al*., "Active Disturbance Rejection Control Using Artificial Neural Network for Dual-Active-Bridge-Based Energy Storage System," *IEEE Journal of Emerging and Selected Topics in Power Electronics*, vol. 11, no. 1, pp. 301-311, 2023,

[80] A. J. Laafou, A. A. Madi, Y. Moumani, and A. Addaim, "Proposed robust ADRC control of a DFIG used in wind power production," *Bulletin of Electrical Engineering and Informatics*, vol. 11, no. 3, pp. 1210–1221, 2022.